Thickness-dependent fcc to bcc structural change in iron films: Use of a 2-ML Ni/W(110) substrate

H. L. Johnston, C. S. Arnold, and D. Venus
Department of Physics and Astronomy, Brockhouse Institute for Materials Research, McMaster University, Hamilton, Canada L8S 4M1
(Received 1 November 1996)

The fcc to bcc structural change in the growth of ultrathin iron films is studied for films grown on a (111) fcc surface, in an attempt to mimic the geometry of the martensitic transition in bulk iron, where the interface is formed from the close-packed planes of the two structures. The use of a 2-ML Ni/W(110) substrate allows good wetting and lattice matching of the iron, without introducing either significant interdiffusion at the interface or a large amount of magnetic material. Low-energy electron diffraction and angle-resolved Auger electron spectroscopy show that the iron films grow as a slightly distorted (111) fcc surface for 3 ML, after which a surface cell intermediate to fcc and bcc appears in a specific Kurjumov-Sachs (KS) orientation. Thicker films show a simultaneous relaxation of the surface unit cell to a bcc structure and the movement of the layer stacking from the fcc position to the KS bcc position. The approximate layer-by-layer evolution of the structure is in marked contast to the complicated growth transition seen for iron films grown on (001) fcc surfaces. This promises to be a useful system to isolate the relation of the structural transition and magnetism, without important contributions from other growth processes. [S0163-1829(97)03219-0]

I. INTRODUCTION

Iron grown as a thin, metastable film upon a face-centered cubic substrate has proven to be a fascinating and complex system for the study of magnetism at surfaces and interfaces, and for the demonstration of the links between film structure, morphology, and magnetism. One factor which contributes to the changes in the magnetic properties of these films as their thickness is increased is the transition from a metastable, epitaxial, fcc-like growth structure to a bcc-like growth structure related to bulk bcc iron. A number of methods, such as the use of surfactants,[1] have been used to stabilize the fcc structure, but for pure, clean iron films, it is difficult to escape the fact that the bcc structure has lower energy and makes a fcc to bcc growth transition inevitable. The relation of this structural change to the magnetic properties of the iron film has been studied extensively for films grown on noble metal substrates, and particularly[2] on Cu(001). Here, as a function of film thickness, one finds sheared face-centered tetragonal growth,[3] a transition fcc region,[4] and finally bcc growth,[5] all with characteristic and fascinating magnetic properties.[6] Unfortunately, the structure and morphology is greatly complicated by the tendency of the iron to mix with the copper substrate,[7] and the film to roughen dramatically as the growth transition occurs.[5,8] It is only through an impressive effort that the contributions of these various issues to the magnetic behavior have been identified and, to some degree, studied systematically. A positive aspect of these works is that Fe/Cu(001) is an ideal system to study the interaction of the many influences on film magnetism; an alternative viewpoint is that it might be fruitful to gain insight through the study of related systems where the magnetic behavior is dominated by a single characteristic of the growth. This has led to initial studies of iron films grown on Ni(001) and Co(001) substrates,[9] where intermixing of the film and substrate are expected to be less serious. For these systems, however, the magnetic properties of the iron film are difficult to study since they may be slaved to the larger net magnetic moment of the substrate, and because it is difficult with many experimental techniques to separate the magnetic response of the iron atoms from that of the substrate atoms. However, even these studies do not address the root of the problem: if one wishes to study the relation between the fcc growth to bcc growth transition on the magnetic properties of the iron film, the (001) surface is a poor choice for the fcc substrate.

The thickness-dependent structural change in iron films has much in common with the phase transition from the fcc structure to the bcc structure in bulk iron, which is a classic example of a first-order martensitic transition.[10] In this diffusionless transition, an interface plane (termed the habit plane) moves through the bulk iron and divides the regions having fcc and bcc structures. These two regions are oriented such that a close-packed $\{111\}_{fcc}$ plane is parallel to a close-packed $\{110\}_{bcc}$ plane. The most likely alignments of the close-packed planes are the Kurjumov-Sachs (KS), where a $\langle 011\rangle_{fcc}$ and $\langle 111\rangle_{bcc}$ direction are parallel, and the Nishiyama-Wasserman (NW), where a $\langle 121\rangle_{fcc}$ and $\langle 101\rangle_{bcc}$ direction are parallel. The habit plane itself is invariant under the structural transformation, a condition which is possible because of the compensatory effects of lattice distortion and shear. The habit plane is often irrational, but in the case of pure iron (up to 0.4% C) the habit plane *is* the close-packed plane. Using the bulk transition as a model, a $(111)_{fcc}$ substrate should result in films where the direction of increasing thickness is normal to the natural habit plane of the bulk transition. This could permit a more continuous growth transition, roughly analogous to a bulk martensitic transition ''in progress,'' with the habit plane ''frozen'' at a certain depth in the film. The essential sound-

ness of this idea is consistent with the scanning tunneling microscopy studies[5,8] of the growth transition of iron films on Cu(001). A very complicated, but patterned, arrangement of defects and shear planes appears at an angle to the surface, and the low-energy electron diffraction (LEED) pattern shows a series of reconstructions related to the shear of the surface layers[3] and the defect patterns.[5] The final Fe bcc phase greatly resembles the close-packed (110) surface in an orientation with respect to the underlying (001) fcc which is not observed for bulk geometries.[11] This process can be thought of as a method by which the natural habit plane for the transition, which is initially at an angle to the surface, can be reestablished normal to the film growth direction.

Choosing a $Cu(111)_{fcc}$ substrate leads again to complications, since the epitaxially grown iron does not wet this surface well, but immediately forms islands[2,12] which undergo the transition to the bcc structure before the islands themselves have properly coalesced. Bauer and van der Merwe[13] have predicted better wetting, lattice matching, and Fe growth on $(111)_{fcc}$ Ni and Co substrates, but these are as yet little studied.[14] Even with these choices, there remain the problems associated with the magnetic characterization of a thin film grown on a magnetic substrate. It is therefore a happy coincidence that Ni is known to grow in a highly ordered (111) fcc structure on a W(110) substrate, even for very thin film thicknesses of two or three monolayers.[15,16] Such a thin Ni buffer layer will continue to have magnetic consequences, but perhaps at least the master/slave relationship between substrate and film will be reversed.

This line of argument has led to the present study of iron films grown on a 2-ML Ni/W(110) substrate, with the aim of discovering a simple example of the fcc to bcc iron growth transition, and with characterizing the structural aspects of that transition. It turns out that one sees a transition dominated by intralayer atomic motions following simple geometric relations, in agreement with the foregoing discussion. This system therefore seems well suited for further studies of the relation of the structural transition and the magnetic properties of iron films.

II. PREPARATION OF THE 2-ML Ni/W(110) SUBSTRATE

The growth of thin Ni films on the W(110) surface has been well characterized in a number of studies.[15,16] The purpose of the present section is to document the method of preparation of the substrate, as the properties of very thin films are much more sensitive to experimental uncertainties than are thick films. Figure 1 shows the geometry of the lattices involved. The solid outline defines a fcc unit cell, and the dashed outlines define two bcc unit cells which are oriented in the NW alignment (to the left of the fcc cell) and one of the KS alignments (below the fcc cell). In this paper, the W(110) single crystal substrate is always aligned as the NW bcc cell in Fig. 1, and all LEED patterns, experimental substrate manipulations, etc., are presented with respect to this orientation in space and on the page. The tungsten crystal was cut and polished to within 0.4° of the $(110)_{bcc}$ surface, and was cleaned before each film deposition by heating to 1800 K in 5×10^{-7} Torr oxygen, and then flashing to 2500 K. This yielded a sharp LEED pattern and carbon contamination levels which were just detectable with a four-grid

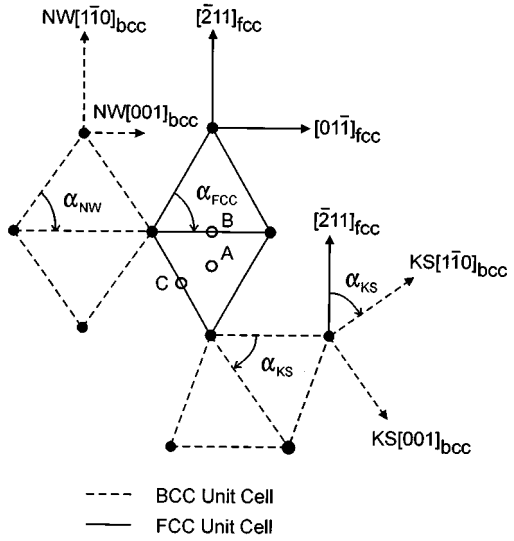

FIG. 1. Relative orientations of the surface unit cells of the substrate and films are illustrated, with the surface normal projecting out of the page. A $(111)_{fcc}$ surface cell is shown by the solid outline, and dashed lines show the NW and KS orientations of the $(110)_{bcc}$ with respect to it. The internal angles α are defined for each cell type. The open circles mark the atomic position of the next layer for a fcc structure (A), a NW bcc structure (B), and a KS bcc structure (C). The $W(110)_{bcc}$ single crystal substrate is aligned as the NW bcc cell.

retardation Auger electron analyzer. Ni was evaporated by electron bombardment of a pure wire, using an evaporator which had an integral flux monitor to ensure a constant deposition rate.[17] The LEED pattern showed initially pseudomorphic growth, then a 7×1 reconstruction along $W[001]_{bcc}$ for thicker films, and finally a sixfold pattern that was very close to hexagonal, with no reconstruction satellite spots—all in agreement with previous results. In accord with these authors, we interpreted the hexagonal pattern as the formation of two stacking domains of the fcc Ni(111) surface, and the 7×1 reconstruction as evidence for the NW relative orientation of the Ni and W unit cells, as illustrated in Fig. 1. For exact matching along the $Ni[2\bar{1}1]_{fcc}$ and $W[1\bar{1}0]_{bcc}$ directions, the Ni cell must be expanded by 3.7% from its bulk lattice constant. Along the $W[001]_{bcc}$ direction, the reconstruction matches nine Ni cells onto seven W cells by contracting the Ni cell by 1.0% from its bulk lattice constant. A matching of this type predicts a distorted fcc cell with internal angle $\alpha_{fcc}=61.14°$, whereas an experimental value of $60.8°\pm0.4°$ was determined for a 2-ML film in the present experiments.

In order to accurately determine the thickness of the Ni layer, Auger electron spectra were recorded as a function of deposition time at room temperature in the energy interval containing the Ni 61-eV and W 48-eV Auger peaks. The spectra were fit using a least-squares criterion to a linear combination of the spectra for the clean W substrate, and a thick Ni film where the W Auger peak was not detectable. The fitting constant for the Ni is plotted in Fig. 2(a) as a function of deposition time. These data were fit in turn to one, two, three, and four linear segments, with a least-squares algorithm free to determine the slopes and intersection points of the lines. The χ^2 from each fit were compared

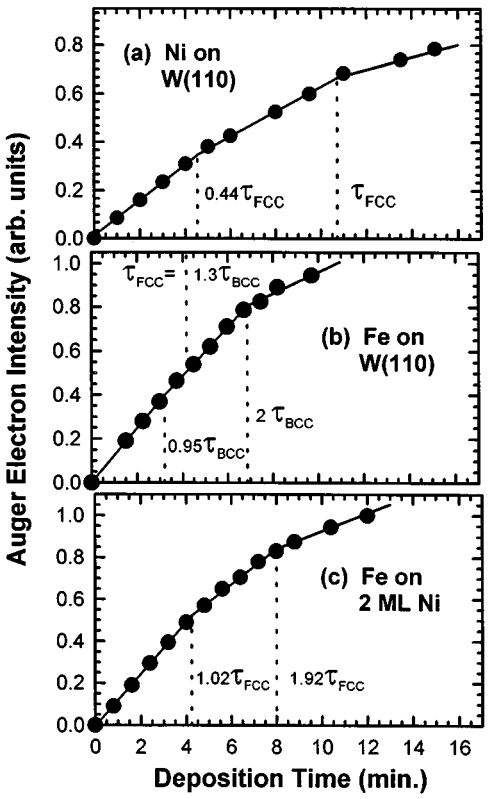

FIG. 2. Intensity of characteristic lines in the Auger electron spectroscopy spectra as a function of the time of metal evaporation. (a) Ni (61 eV) deposited on W(110). (b) Fe (47 eV) deposited on W(110). (c) Fe (47 eV) deposited on 2-ML Ni/W(110). The lines and labeled times τ are unconstrained, linear least-squares fits to linear segments and are discussed in the text.

using the f test, which takes into account the reduction in degrees of freedom as the number of linear segments is increased. The statistical analysis suggests that the Ni Auger uptake curve is best represented by three linear segments, where there is a first weak slope change at the deposition time $0.44\tau_{\mathrm{fcc}}$ and a stronger slope change at τ_{fcc}. The labeling of these times reflects our interpretation of the stronger slope change as the completion of the reconstructed monolayer, and the weaker slope change as associated with the end of pseudomorphic growth. (The LEED reconstruction was first visible at about $0.6\tau_{\mathrm{fcc}}$.) These results are in detailed agreement with those of Kolaczkiewicz and Bauer,[15] with even the ratios of the slopes at the slope changes (0.70 and 0.53) being in quantitative agreement. These data confirm the very good wetting of W(110) by Ni, and serve to calibrate the Ni film thickness to within ± 0.1 ML.

The very low solubility of most metals in W permits films to be annealed without causing intermixing at the interface. Experimentation showed that the LEED pattern of the Ni film was improved when the films were grown at an elevated temperature, and that this did not affect the Auger electron intensities. All the Ni/W(110) substrates in this study were thus prepared by growing the first monolayer at a substrate temperature of 550 K and subsequent layers at 390 K. The LEED pattern for a 2-ML Ni film then had a sharp hexagonal pattern of spots, and more diffuse reconstruction spots which were significantly weaker than those observed for the monolayer.

III. GROWTH OF fcc Fe ON 2-ML Ni/W(110)

Since preliminary studies showed that growing Fe directly on 1-ML Ni/W(110) led quickly to a very diffuse LEED pattern, a 2-ML Ni film was chosen as the thinnest practical magnetic substrate. The Fe evaporator was calibrated by LEED and Auger experiments of deposition directly onto the W(110) surface at room temperature. This system is known to produce a series of distinctive LEED patterns with increasing coverage, which were reproduced in the present studies.[18] Data for the Fe Auger uptake curve are plotted in Fig. 2(b), following the same analysis procedure described for the Ni deposition. Once again, according to the f test, the data are best represented by three linear segments. The first, very weak change in slope has also been observed by Gardiner[19] (the ratios of slopes at these changes, 0.89 and 0.45, are in quantitative agreement with those measured by Gardiner), but is too subtle for calibration purposes. The characteristic feature of this curve in previous studies at room temperature is the stronger second slope change, which has been shown to represent the completion of the Fe bilayer[20] on W(110). This feature is therefore interpreted as $2\tau_{\mathrm{bcc}}$, and it is then found that the first slope change occurs at $0.95\tau_{\mathrm{bcc}}$. Using this calibration, the ratio of the areal atom densities on the W(110) and Ni(111) surfaces gives a time for the deposition of Fe equivalent to one pseudomorphic layer on Ni(111) as $\tau_{\mathrm{fcc}}=1.3\tau_{\mathrm{bcc}}$. [Of course, this τ_{fcc} is different than that in Fig. 1(a), since a different evaporator is being calibrated.] A similar Auger intensity experiment was then performed for Fe deposition at room temperature on 2-ML Ni/W(110), the results being presented in Fig. 2(c). The same analysis leads to three linear segments, with the unconstrained positions of the slope changes fit to $1.02\tau_{\mathrm{fcc}}$ and $1.92\tau_{\mathrm{fcc}}$ in terms of the *independent* calibration of τ_{fcc} in Fig. 2(b). This is internally consistent evidence that the Fe wets the Ni film well, grows pseudomorphically on the strained fcc template, and that in the initial stages at least the growth mode is approximately layer by layer. The thickness of the Fe films in ML in this paper will therefore refer to the calibrated amount of material deposited in τ_{fcc}.

A final Auger electron spectroscopy experiment was performed to gain insight into the amount of intermixing of the Fe into the Ni film. 0.8-ML of Fe was deposited onto 2-ML Ni/W(110), and Auger spectra were recorded (close to room temperature) as a function of annealing temperature. The low-energy region of the spectrum was fit to a linear combination of the Auger spectra of 2-ML Ni/W(110) and a very thick Fe film. The higher-energy region was fit to a single, clean W Auger spectrum. The resulting fitting constants are plotted in Fig. 3, where the lines are guides to the eye. The W Auger intensity stays rather constant until an annealing temperature of 550 K, where it begins to increase. This is interpreted as the onset of significant islanding of the film, probably as islands on top of a single monolayer which is tightly bonded to the W surface. The Fe and Ni signals, however, change rather linearly starting immediately at the lowest annealing temperature. This is interpreted as intermixing of the Fe and Ni, and the lack of plateau at low annealing temperatures suggests that some intermixing has already occurred in the film as deposited. It is difficult to quantify the amount of intermixing from this experiment, but

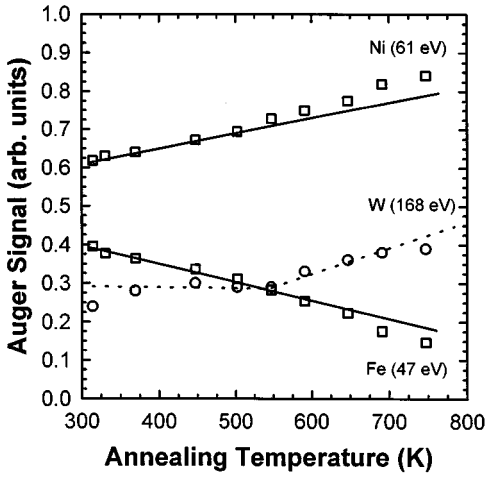

FIG. 3. Intensity of characteristic lines in the Auger electron spectroscopy spectra for a 0.8-ML Fe/2-ML Ni/W(110) film, which was grown at room temperature, and annealed to successively higher temperatures. The lines are guides for the eye.

it is clearly a gradual process: annealing to 360 K, for instance, makes only a small change in the Auger intensities. Because of this, and because the Ni film is grown at slightly elevated temperature, the effect of growing the Fe film at slightly elevated temperature (360 K) was investigated. This led to an improvement in the sharpness of the LEED pattern, and this growth temperature was therefore adopted for all subsequent films.

The structure of the Fe films was investigated using LEED patterns and angle-resolved Auger electron spectroscopy (ARAES). Initially, deposition of Fe on 2-ML Ni/W(110) led to no important changes in the LEED pattern observed for the 2-ML Ni film. The sharpness of the spots was at first degraded, but then improved again, so that at 3 ML of Fe, a sharp hexagonal LEED pattern with no reconstruction was obtained. This is illustrated in Fig. 4, for a primary energy of 96 eV. An internal angle $\alpha_{\mathrm{fcc}}=60.8°\pm0.4°$ was measured from photographs of the pattern, and the lack of threefold symmetry again indicates that there are domains of two stacking sequences present.

The angle-resolved Auger experiments[21] are illustrated

FIG. 4. Photograph of the LEED pattern of 3-ML Fe/2-ML Ni/W(110), for a primary beam energy of 96 eV. The orientation of the tungsten substrate and Ni film in direct space is as the NW unit cells in Fig. 1.

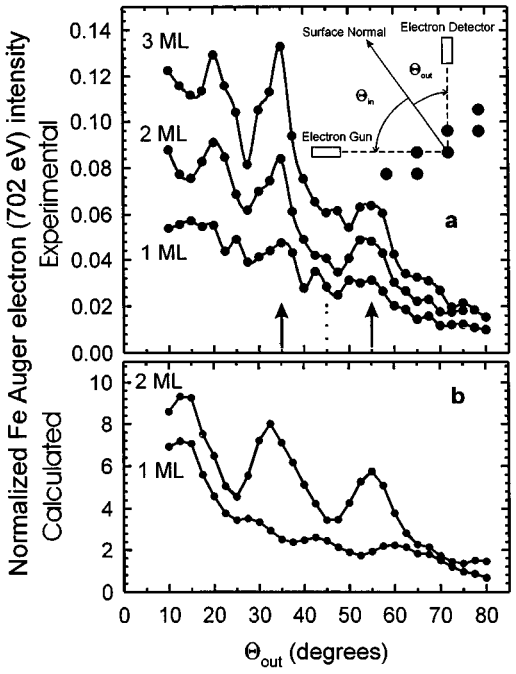

FIG. 5. Angle-resolved Auger electron spectroscopy (ARAES) traces for Fe films on 2-ML Ni/W(110). The experimental geometry is illustrated in the inset. (a) Experimental results for 1-, 2-, and 3-ML Fe films. The expected angles for forward-focusing by a fcc surface cell in the NW orientation (arrows), and by a bcc surface cell aligned with the W substrate (dotted line) are marked. The curves are normalized to the same incoming primary beam flux. (b) The calculated traces for a 1- and 2-ML Fe film with a fcc surface cell in the NW orientation. Both incoming and outgoing focusing conditions are included, as discussed in the text.

schematically in the inset to Fig. 5(a). High-energy Auger electrons are, to a good approximation, emitted isotropically by an excited atom, but the angular distribution of the Auger electrons can be perturbed if the emitting atom is in a crystalline environment. The trajectories of the electrons passing close to a positive ion core can be deflected towards the ion core, causing a focusing of the Auger electrons along the crystallographic directions where the ion cores are situated. This forward-focusing effect is strongest in very thin films where multiple forward-scattering interactions are not geometrically possible,[22] and is observed primarily along the directions where nearest neighbors lie. In the present experiments, the films were rotated about the NW$[001]_{\mathrm{bcc}}$ direction of the W crystal illustrated in Fig. 1 (this is equivalent to the $[011]_{\mathrm{fcc}}$ direction of the 2-ML Ni). Assuming the fcc stacking position marked ''*A*'' in Fig. 1, the geometry illustrated in the inset to Fig. 5(a) is obtained, and forward focusing at $\Theta_{\mathrm{out}}=35°$ is expected. Assuming the alternate fcc stacking position in the upper half of the fcc unit cell in Fig. 1 predicts a peak in the ARAES at $\Theta_{\mathrm{out}}=55°$. Assuming a bcc structure in the orientation of the NW orientation of the W substrate predicts a peak at $\Theta_{\mathrm{out}}=45°$.

The ARAES experiments were performed with a fixed angle between the incoming primary, 2000-eV electron beam and the entrance aperture of the electron energy analyzer, such that $\Theta_{\mathrm{in}}+\Theta_{\mathrm{out}}=90°$. The angular resolution of the electron optics was $\pm2°$. In order to compensate for the

possible drift of the electron gun current, the electron count was recorded in a rapid series of interleaved time steps at the peak energy of the Fe (702 eV) Auger electrons, and two positions suitable for extrapolating a linear background. The ARAES data were then evaluated as the ratio of the Auger peak counts minus the background, all normalized to the background. While this method removed spurious temporal drifts, it introduced an arbitrary scale of normalization. This was removed by constructing the average, angle-resolved inelastic background as measured in many ARAES experiments. Since this function was found to be smoothly varying and had little scatter, it was fit to a polynomial, and the resulting function was multiplied times the normalized ARAES spectra to give the angular dependence of the Fe Auger electrons alone, normalized to constant exciting beam current. These data are shown in Fig. 5(a) for 1-, 2-, and 3-ML Fe films grown on 2-ML Ni/W(110). The spectra for 2- and 3-ML Fe show clear peaks at $\Theta_{\rm out}=35°$ and 55°, and no discernible peak at 45°, indicating that two stacking domains of fcc iron are present (in agreement with the LEED pattern), but that bcc iron is not present. Small peaks may also be present at the fcc forward-focusing angles for the 1-ML Fe film. Since the Fe emitter must be below another atom to produce forward-focused electrons, the size of these peaks is a measure of the imperfection of the Fe films due to a combination of mechanisms: (i) the degree to which the 2-ML Ni substrate contained regions of 1-ML thickness, (ii) the uncertainty in the Fe film thickness, and (iii) the amount of intermixing of Fe into the Ni film. The data are evidence that none of these effects is serious.

For quantitative calculations of Auger electron forward focusing, the ARAES spectrum from a single emitter at a particular lattice site n is denoted $I_{\rm out}(\Theta_{\rm out},n)$, and may be calculated by assuming that an isotropic, outgoing electron wave is scattered elastically by an array of atoms, where only independent, single-scattering events are considered.[23] The scattered amplitudes far from the array are summed and the scattered intensity is computed. The present experimental geometry is complicated by the fact that the incoming electron beam may also experience forward focusing. This can be seen in the inset to Fig. 5(a), where the beam from the electron gun may be focused by a first-layer atom onto a second-layer atom, so that the latter experiences a greater excitation probability at $\Theta_{\rm in}=55°$ than at other angles. The incoming focusing $I_{\rm in}(\Theta_{\rm in},n)$ may be calculated by the same method as $I_{\rm out}(\Theta_{\rm out},n)$, by using time-reversal symmetry[24] and a transformation of variables.[25] The observed angular dependence of Auger emission from a particular atom will then be the product of these two. Finally, the contribution from all atoms must be normalized to the same scale, and summed. The calculation described thus far is normalized ''per Auger electron generated at site n.'' The relative probabilities of excitation of atoms in different lattice sites is given by the relative energy dissipation at these sites. A first approximation to this function is given by the phenomenological attenuation of the primary beam.[26] This varies exponentially from layer to layer, and as $1/\sin\Theta_{\rm in}$ within each layer as the primary beam approaches glancing incidence. Taking these together, the experimental situation is described by

$$I_{\rm net}(\Theta_{\rm out})=\sum_n I_{\rm in}(\Theta_{\rm in},n)I_{\rm out}(\Theta_{\rm out},n) \times\exp[-d(n)/(\lambda\,\sin\Theta_{\rm in})]/\sin\Theta_{\rm in}, \quad (1)$$

where $d(n)$ is the perpendicular depth of the lattice site from the surface, and λ is the inelastic attenuation depth. Single-scattering calculations were carried out using the program SSC, developed by Friedmann and Fadley,[23] with scattering phase shifts calculated in the program FEFF, developed by Rehr, Albers, and Mustre de Leon.[27] These are presented in Fig. 5(b) for the cases of 1- and 2-ML Fe films, where the single-scattering assumption is strictly valid. The index n was summed over the two inequivalent positions in both possible fcc stacking sequences. The agreement between the measured and calculated spectra is very good, and confirms the fcc structure of the Fe. It also permits a more detailed understanding of three important points: (i) the rising ''background'' as $\Theta_{\rm out}$ becomes smaller is a true effect which results from increased energy deposition in the surface region at glancing angles of primary electron incidence; (ii) the same mechanism enhances the intensity of peaks at small emission angles relative to those at large emission angles—thus the peaks at 35° and 55° due to equal amounts of the two fcc stackings are not equal in height; (iii) in the present geometry the appearance of the characteristic peaks at 35°, 45°, and 55° is not affected by the forward scattering of the incoming beam, because in all three cases, the incoming and outgoing beams experience forward focusing at equivalent geometries. At very low emission angles, however, the enhanced sensitivity can lead to prominent peaks due to second-order focusing (as between 15° and 20°) which complicate a qualitative interpretation.

In conclusion, the Auger uptake curves, LEED, and ARAES measurements are a self-consistent data set which indicate that up to 3 ML Fe grows on the 2-ML Ni/W(110) substrate as two domains of a slightly distorted $(111)_{\rm fcc}$ surface with different stacking sequences, which are epitaxial to the Ni film.

IV. fcc TO bcc TRANSITION FOR Fe/2-ML Ni/W(110)

The first indications of the growth of bcc Fe are given by LEED patterns recorded for 4-ML Fe films. Figure 6(a) shows the pattern for a primary energy of 96 eV, and Fig. 6(b) gives a schematic interpretation. Four of the six bright spots associated with the distorted fcc Fe have split into triplets, so that the twofold symmetry of the pattern is more pronounced. Variation of the primary energy shows that the upper spots on the left are correlated with the lower spots on the right, and vice versa. Figure 6(b) shows that these new spots can be represented as a superposition of two domains of bcc-like unit cells in an orientation which is given by the KS orientation in Fig. 1. Two qualitative features are worth particular attention. First, the observed KS orientations represent only two of the six possible such orientations.[28] The 3-ML Fe films show a distortion equivalent to that seen for the 7×1 reconstructed Ni films, where there is a 3.7% expansion along $[\underline{2}\overline{1}1]_{\rm fcc}$ and a 1.0% compression along $[0\underline{1}1]_{\rm fcc}$. Using the nearest-neighbor distance for bulk Fe,

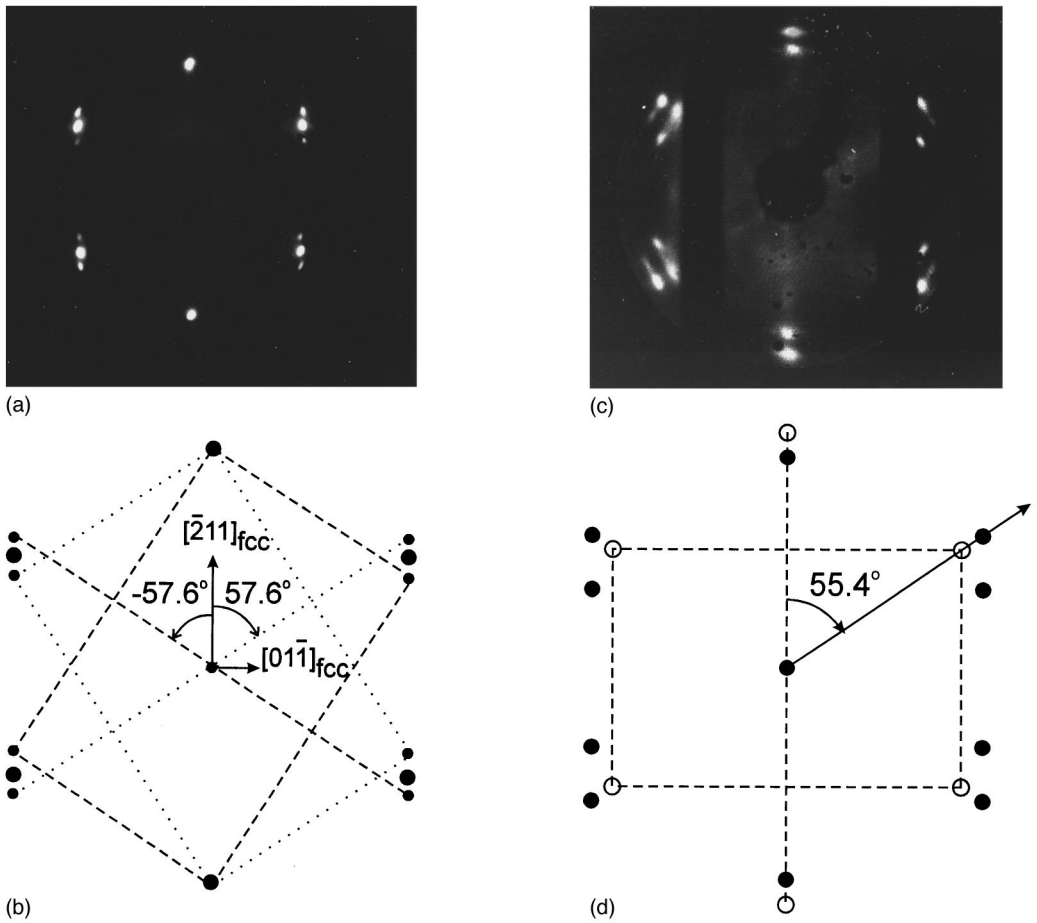

FIG. 6. LEED patterns at a primary beam energy of 96 eV for thicker Fe films grown on 2-ML Ni/W(110). LEED pattern (a) and schematic (b) are for a 4-ML Fe film. The schematic shows two distorted bcc surface cells in the KS orientation of Fig. 1. LEED pattern (c) and schematic (d) are for a 12-ML Fe film. The schematic shows, using open circles, a slightly distorted bcc surface cell in the NW orientation of Fig. 1.

the observed KS orientation represents a 0.7% compressive strain along the $[011]_{fcc}$ matching direction, whereas matching along the nominal $[101]_{fcc}$ or $[110]_{fcc}$ directions would require a 2.9% expansion. (A NW orientation requires a 10.4% expansion.) A rigid model therefore shows a clear reduction of strain energy for the observed KS orientations. Second, the new spots represent a distorted bcc-like cell, since the internal angle α_{KS} defined in Fig. 1 is equal to $\pm 57.6°$ instead of the true bcc value of $\pm 54.7°$. The observed distortion allows the bcc-like cell to maintain registry with the fcc underlayers in the $[110]_{fcc}$ direction in direct space, as can be seen by the horizontal alignment of the spots in Fig. 6(a). This arrangement presumably reduces the energy of interlayer interaction.

LEED patterns of thicker films show a fading of the fcc spots, and an evolution of the bcc-like KS unit cells to smaller values of α_{KS}. A new qualitative feature is seen first for 8-ML Fe films. It is illustrated in a 12-ML Fe film in Fig. 6(c), where it is fully developed. The fcc spots are now absent, but six new spots are present (two are hidden in the photograph by the shadows cast by a Helmholtz coil arrangement near the sample holder). The new spots are indicated as open circles in the schematic representation in Fig. 6(d). They can be represented as a bcc-like cell in the NW configuration in Fig. 1, with internal angle $\alpha_{NW}=55.4°$. The figure also shows that the original KS cells have evolved such that α_{KS} is also equal to 55.4°, so that the entire LEED pattern can be represented as the incoherent superposition of three equivalent bcc-like cells: two KS cells rotated $\pm 55.4°$ from a NW cell, all referenced to the underlying fcc Fe. It is not clear why the emergence of domains of the NW orientation is favorable, other than to note that they occur on the bcc-like surface (not on the fcc surface), and then only once the internal angle α_{KS} has obtained a value close to that of a true bcc cell. The particular NW orientation which appears is the only one that preserves the twofold symmetry of the original, distorted fcc surface. It may be that this orientation nucleates at the boundaries where the different KS domains meet.

The evolution of the bcc cells measured from photographs of LEED patterns is summarized in Fig. 7, where the internal angles α for both orientations are presented as a function of film thickness. The internal angle of the fcc cell is also shown for those thicknesses where it is observed. This plot is very suggestive of a fcc to bcc transition in three distinct steps. The first is the sudden appearance of a structure intermediate to fcc and bcc in the KS orientation, followed by a gradual relaxation of the surface unit cell to that of a bcc structure. Finally, identical bcc cells nucleate in the NW orientation. The evidence for the gradual relaxation of the KS

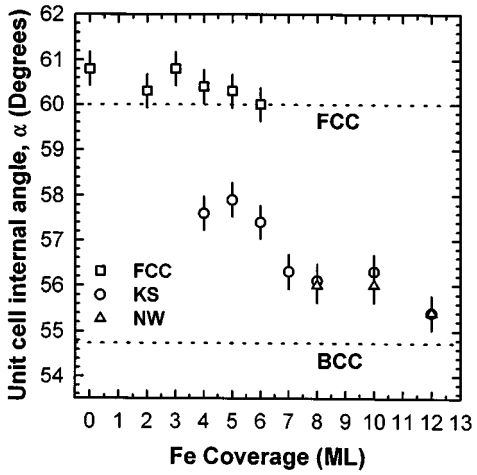

FIG. 7. Internal angles α (defined in Fig. 1) of the different surface unit cells, measured from photographs of LEED patterns, as a function of the Fe film thickness. The dashed lines show the expected angles for the fcc and bcc structures.

cells is particularly intriguing. LEED at a primary energy near 100 eV should measure a weighted average of the structure of the first few atomic layers, giving the smearing of the spots in Fig. 6 perpendicular to the radial direction—that is, along the direction the spots move with changing film thickness. The fact that the spots do not degrade into a continuous arc, but rather remain relatively well defined and show measurable dispersion, suggests that the bcc iron is not growing as rough islands which expose many layers with a range of α_{KS}, but rather continues to follow approximately layer growth, with each layer having a unit cell which is incrementally relaxed from the previous layer. This is further supported by the rapid disappearance of the fcc LEED spots.

As the surface unit cell distorts continuously towards a bcc structure, the potential minimum inside the cell is expected to shift from the fcc stacking position, labeled by ''*A*'' in Fig. 1, to one of the bcc stacking positions labeled ''*B*'' and ''*C*'' in Fig. 1. Since the layer spacing between bulk close-packed fcc and bcc planes is the same (when measured in units of the nearest-neighbor distance), no change in the interlayer spacing is expected. In order to investigate the stacking of the surface unit cells, a series of angle-resolved Auger experiments were conducted for films showing the transition to bcc Fe. These are presented in Fig. 8(a). The extended lines on the *y* axis show the amount by which successive curves have been displaced to avoid overlapping. In overview, the data first show a dispersion of the peaks from the fcc angles of 35° and 55° to smaller and larger angles, respectively, as the films get thicker. The latter peak becomes significantly weaker, appearing as a shoulder. Then, for 12-ML Fe films, there is a complete change in character, with a very strong peak occurring at 45°.

These curves may be interpreted by comparison to the calculated ARAES spectra for different stacking positions of the layers along the lines *AC* or *AB* in Fig. 1. Since the single-scattering theory is strictly valid for films only 1 or 2 ML thick, and since the most prominent structure is expected to arise from simple, forward focusing by nearest-neighbor atoms, the following approximate method has been adopted. A two-layer system is formed from a bottom layer with a

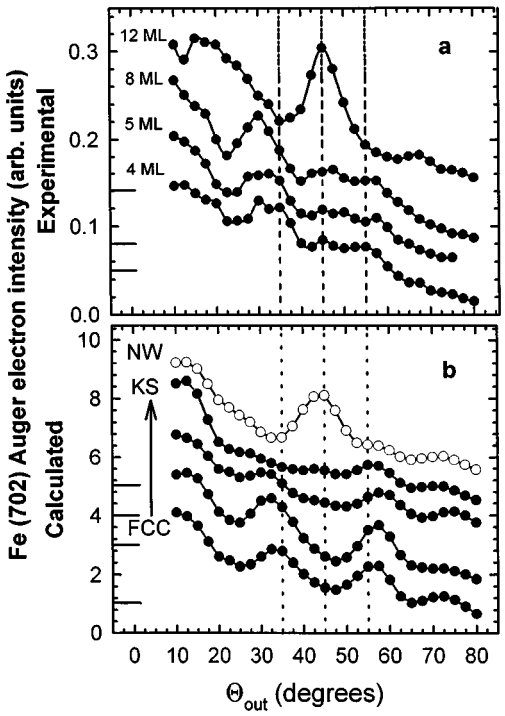

FIG. 8. Angle-resolved Auger electron spectroscopy traces for thicker Fe films. (a) Experimental results, where successive curves have been displaced an amount indicated by the extended lines on the *y* axis. (b) Calculated curves for different stacking positions of an Fe layer formed from the KS bcc-like surface unit cells of a 4-ML film, on top of a fcc unit cell for the 3-ML film. The filled symbols are for stacking positions along the line *AC* in Fig. 1. The open symbols are for the stacking position *B* in Fig. 1. Successive curves have been displaced an amount indicated by the extended lines on the *y* axis.

true fcc Fe structure, and a top layer in the intermediate KS structure given by the LEED pattern in Fig. 6(a). The interlayer distance is assumed to be constant at the distance common to the close-packed planes in both fcc and bcc bulk structures. Calculations made according to Eq. (1), for different layer stacking sites along the lines *AB* and *AC*, are presented in Fig. 8(b). The solid symbols represent the calculations for a progression of the stacking site along *AC*, from the fcc site to the KS bcc site. The open symbols represent the calculation at the end-point stacking site *B* for the NW bcc structure. Because of the neglect of contributions from atoms deeper than the second Fe layer, the calculated peak heights are not as reliable as the peak positions. There is an impressive agreement with the evolution of the calculated and experimental spectra. The calculated peak positions are summarized in Fig. 9. The ARAES experiments up to 8-ML-thick Fe films are well represented by the calculations for movement of the stacking position from the fcc to the KS bcc site. The approximate nature of the calculation and the width of the experimental peaks make a more precise correlation of stacking position against film thickness unreliable. For the 12-ML Fe films, the experiments are in good agreement with the calculation for stacking at the NW bcc site.

These results give strong support to a description of fcc to bcc transition in these films as a layer-by-layer evolution of the surface cells in both shape and stacking position. The

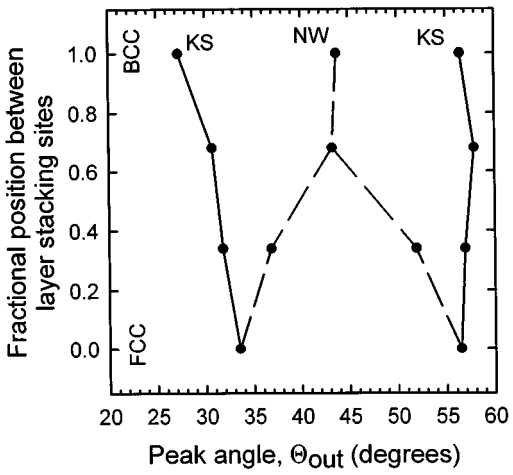

FIG. 9. Positions of the forward-focusing peaks in the calculated ARAES traces (as in Fig. 8) as a function of the stacking position along the line AC in Fig. 1 (ending in the KS bcc stacking position) and along the line AB in Fig. 1 (ending in the NW bcc stacking position).

ARAES and LEED studies are internally consistent, with the stacking position moving toward the KS bcc site as the surface unit cell relaxes to two domains of the true bcc structure in the KS orientation. Only when this process is nearly complete does the LEED show the appearance of the NW bcc domains, in agreement with the strong peak at 45° in the ARAES at these thicknesses. The experimental ARAES spectrum for the thickest film (12 ML) is in fact well represented by a summation of the calculated curves for the KS and NW stacking sites, since the calculation for the KS site shows little structure. The details of the emergence of the NW bcc domains remains unexplained, as it is not clear how this unit cell can be accommodated to the existing KS bcc growth without a significant distortion which is not observed in the LEED pattern. To our knowledge, the fcc to bcc structural changes in ultrathin Fe films grown on $(111)_{fcc}$ surfaces studied so far show either a KS or NW orientation, but not both.[28,29] Some studies of thick Fe films (of order 100 ML) grown on a Ni(111) single crystal show a combination of KS and NW domains,[14] but this seems to correspond to a loss of epitaxy to the substrate, since all possible configurations are present.

V. DISCUSSION

Insofar as the experimental methods used in these studies can detect, Fe films grown on 2-ML Ni/W(110) show a simple fcc to bcc growth transition, with evolution of the structure in the direction of film growth. This is accomplished by the nucleation of surface unit cells in the KS orientation which are midway between fcc and bcc, followed by the incremental evolution of the shape and stacking position of the cells to that of true bcc. The present studies give no direct indication of the film morphology, but the continuous evolution of the LEED and ARAES measurements suggest that the film growth in the transition region is not rough, but rather exposes only a few layer thicknesses at any time. This type of incremental structural transition is unusual in that the bcc structure does not seem to be introduced as defects which reduce the in-plane strain of the film, while leaving the structure of the fcc and bcc portions fixed. Scanning tunneling microscopy (STM) and reflection high-energy electron diffraction studies of the growth of these films would provide a most welcome test of these conclusions. The STM experiments may have difficulty in detecting the growth transition itself, since the layer spacing of the fcc and bcc structure is expected to be very nearly the same.

It is interesting to speculate on the rough analogy between the growth transition in these films and the martensitic phase transition in bulk Fe. In the first place, the present finding of a simple transition with a planar geometry supports the use of a film geometry where the surface lies parallel to the habit plane in the bulk transition. These experiments show at first a discontinuous change in the surface unit cell (as would be expected in an analogous first-order phase transition), followed by an incremental relaxation of the unit cell, as might be foreseen for a ''frozen'' martensitic transition front. The most analogous metallurgical situation would seem to be the interfaces of finite, metastable martensitic particles in bulk materials. Recent electron microscopy studies of Cu precipitates in a bcc Fe matrix show a series of epitaxial relationships, depending on particle size.[30] Interfaces analogous to planar films are found for particles >17 μm, where an untwinned, distorted fcc structure close to the KS orientation is found. Growth of the particle finally leads to a fcc structure in the KS orientation for particle sizes greater than 40 μm. While these studies of precipitates are of a bcc to fcc martensitic transition (the reverse of the present film studies), in both cases there is a gradual, epitaxial accommodation as the relative importance of the interface is decreased because the particle/film grows larger/thicker.

Finally, it appears that the use of the 2-ML Ni/W(110) substrate provides a tractable experimental system for the study of the magnetic behavior of Fe films as they undergo the fcc to bcc growth transition. Despite the extreme thinness of the Ni buffer layer, epitaxial fcc Fe films with little intermixing are produced up to a thickness of 3 ML. The slightly distorted fcc unit cell further simplifies the growth transition by causing a preferred orientation among the many possible KS alignments. There is hope that the Ni will not dictate the magnetic properties of the Fe film, except perhaps in the interesting region of $\leqslant 1$ ML Fe. These and other magnetic studies are currently underway.

ACKNOWLEDGMENTS

We are pleased to acknowledge the technical assistance of M. Kiela. We thank G. Purdy for a critical reading of the manuscript. This work has been supported by the Natural Sciences and Engineering Research Council of Canada. H.L.J. and C.S.A. gratefully acknowledge support from the government of Ontario.

[1] A. Kirilyuk, J. Giegiel, J. Shen, and J. Kirschner, Phys. Rev. B **52**, 11 672 (1995).
[2] Extensive references are found in M. T. Kief and W. F. Egelhoff, Jr., Phys. Rev. B **47**, 10 785 (1993).
[3] J. V. Barth and D. E. Fowler, Phys. Rev. B **52**, 11 432 (1995).
[4] M. Wuttig and J. Thomassen, Surf. Sci. **282**, 237 (1993).
[5] M. Wuttig, B. Feldmann, J. Thomassen, F. May, H. Zillgen, A. Brodde, H. Hannemann, and H. Neddermeyer, Surf. Sci. **291**, 14 (1993).
[6] J. Thomassen, F. May, B. Feldmann, M. Wuttig, and H. Ibach, Phys. Rev. Lett. **69**, 3831 (1992); D. P. Pappas, C. R. Brundle, and H. Hopster, Phys. Rev. B **45**, 8169 (1992); D. Li, M. Freitag, J. Pearson, Z. Q. Liu, and S. D. Bader, Phys. Rev. Lett. **72**, 3112 (1994).
[7] D. A. Steigerwald, I. Jacob, and W. F. Egelhoff, Jr., Surf. Sci. **202**, 472 (1988).
[8] J. Giergiel, J. Kirschner, J. Landgraf, J. Shen, and J. Woltersdorf, Surf. Sci. **310**, 1 (1994); J. Giergiel, J. Shen, J. Woltersdorf, A. Kirilyuk, and J. Kirschner, Phys. Rev. B **52**, 8528 (1995).
[9] W. L. O'Brien and B. P. Tonner, Phys. Rev. B **52**, 15 332 (1995); E. J. Escoria-Aparicio, R. K. Kawakami, and Z. Q. Qiu, J. Appl. Phys. **79**, 4964 (1996).
[10] A simple introduction is L. Delaey, in *Materials Science and Technology*, edited by R. W. Cahn, P. Haasen, and E. J. Kramer (VCH, New York, 1991), Vol. 5.
[11] W. Pitsch, Philos. Mag. **4**, 477 (1959).
[12] A. Brodde and H. Neddermeyer, Ultramicroscopy **42-44**, 556 (1992).
[13] E. Bauer and J. H. van der Merwe, Phys. Rev. B **33**, 3657 (1986).
[14] J. Echigoya, M. Nemoto, and H. Suto, Trans. Jpn. Inst. Met. **21**, 99 (1980).
[15] J. Kolaczkiewicz and E. Bauer, Surf. Sci. **144**, 495 (1984).
[16] K.-P. Kamper, W. Schmidt, G. Güntherodt, and H. Kuhlenbeck, Phys. Rev. B **38**, 9451 (1988).
[17] T. Jones, J. Sawler, and D. Venus, Rev. Sci. Instrum. **64**, 2008 (1993).
[18] U. Gradmann and G. Waller, Surf. Sci. **116**, 539 (1982).
[19] T. M. Gardiner, Thin Solid Films **105**, 213 (1983).
[20] M. Przybylski, I. Kaufmann, and U. Gradmann, Phys. Rev. B **40**, 8631 (1989).
[21] W. F. Egelhoff, Jr., in *Ultrathin Magnetic Structures I*, edited by J. A. C. Bland and B. Heinrich (Springer, Berlin, 1994).
[22] A. P. Kaduwalla, D. J. Friedmann, and C. S. Fadley, J. Electron Spectrosc. Relat. Phenom. **57**, 223 (1991).
[23] D. J. Friedmann and C. S. Fadley, J. Electron Spectrosc. Relat. Phenom. **51**, 689 (1990).
[24] S. Chambers, Adv. Phys. **40**, 357 (1991).
[25] S. Chambers, J. M. Vitomiron, and J. H. Weaver, Phys. Rev. B **36**, 3007 (1987).
[26] Y. Gao and J. Cao, Phys. Rev. B **43**, 9692 (1991).
[27] J. J. Rehr, A. C. Albers, and J. Mustre de Leon, Physica B **158**, 417 (1989).
[28] U. Gradmann and P. Tillmanns, Phys. Status Solidi A **44**, 539 (1977); D. Tian, F. Jona, and P. Marcus, Phys. Rev. B **45**, 11 216 (1992).
[29] B. Voigtlander, G. Meyer, and N. U. Amer, Surf. Sci. **255**, L529 (1991); S. Andrieu, M. Piecuch, and J. F. Bobo, Phys. Rev. B **46**, 4909 (1992).
[30] P. S. Othen, M. L. Jenkins, and G. D. W. Smith, Philos. Mag. A **70**, 1 (1994).